Proc. ECIO 2007, 25-27 April, 2007, Copenhagen, Denmark, paper FA1
(note: door een drukfout staat er boven het paper ten onrechte FA2)

Focused Ion Beam Milling Strategies of Photonic Crystal Structures in Silicon

Wico C.L. Hopman (1), Feridun Ay (1), Wenbin Hu (1), Vishwas J. Gadgil (1),
Laurens Kuipers (2), Markus Pollnau (1), René M. de Ridder (1)
1) MESA+ Institute for Nanotechnology, University of Twente, P.O. Box 217, 7500 AE Enschede, The Netherlands,
W.C.L.Hopman@utwente.nl, F.Ay@utwente.nl, R.M.deRidder@utwente.nl
2) FOM Institute for Atomic and Molecular Physics (AMOLF), Kruislaan 407, 1098 SJ Amsterdam, The Netherlands

Abstract: *We report on optimisation of the side wall angle of focused ion beam (FIB) fabricated sub-micron diameter holes in silicon. Two optimisation steps were performed. First, we compare two different FIB scanning procedures and show the advantages of using a spiral scanning method for the definition of holes in photonic crystal slab structures. Secondly, we investigate the effect on the geometry, of parameters such as dwell time, loop number, and ion dose, to determine the optimum FIB milling parameters for reducing the tapering effect. Furthermore, we report on the initial results regarding effects of Ga^+ ion implantation during FIB milling on optical losses, both before and after an annealing step, showing over a decade reduction of optical loss.*

Introduction

Photonic crystal slabs (PCS) have recently received much attention as an attractive technology promising an increase of photonic integration density by several orders of magnitude [1, 2]. In a typical PCS, in-plane light confinement is realised by the photonic bandgap effect, while the vertical confinement is a result of refractive index guiding. A high-refractive index layer (e.g. Si) perforated with a 2-D periodic lattice of air holes constitutes a characteristic PCS structure, having structural detail in the sub-micrometre range.

For fabrication of the PCS structures small photonic crystal elements requiring sub-10 nm resolution have to be aligned with relatively large-sized features like access waveguides for interfacing with the outside world. Focused ion beam (FIB) milling is a very interesting tool for achieving both of these requirements simultaneously. FIB processing is a well-established technique with unique capabilities to locally sputter-etch, ion-implant, and deposit metals and insulators with a feature size in the order of nanometres, without the need of a mask [3, 4].

Despite the maturity of this method for e.g. semiconductor chip repair, the realisation of photonic components with desired characteristics is still challenging. In particular, fabricating sub-micron holes in silicon with perfectly vertical side-walls by FIB milling is nearly impossible due to the redeposition effect [5]. In addition, the losses induced by ion bombardment and implantation of for example gallium ions in the sample, causing modifications of the crystalline Si, are still too high to fabricate practical PCS devices [6]. These issues are addressed in the following sections.

Experimental

The FIB experiments presented in this paper were conducted on the dual-beam Nova 600 FIB machine from FEI company. The advantage of this machine is that it contains both an electron and ion beam in a single vacuum chamber. Therefore, nanostructuring by FIB milling and inspection by SEM can be done in a single session. The machine uses a liquid gallium source to generate a Ga^+ ion beam. The stitching-error-free writing field of the FIB is divided in 4096 by 4096 pixels. The actual size of the writing field depends on the selected magnification (compared to the size on the monitor). In the experiments reported here, we fixed the magnification to 5000 times, resulting in a writing field of about 25x25 μm and a grid spacing of 6.2 nm. This writing field size is well suited for definition of PCS devices on top of larger structures like waveguides which can be defined using conventional UV lithography. The machine allows for a number of currents to be selected, ranging from 1.5 pA to several nanoamperes. However switching between currents requires time-consuming switching of apertures and refocusing. Therefore the milling current was fixed at 48 pA and the acceleration voltage was set to 30 kV. The minimum obtainable beam spot-size is determined by the milling current. At 48 pA the 1/e spot size was estimated to be 18 nm. The ion beam can be controlled by a so-called stream-file containing the sequential coordinates defining the scan path, and the dwell time at each of these coordinates. The structures were defined such that the 1/e ion beam spot size was maintained at approximately 1.5 times the inter-pixel distance.

Cross-sectioning

FIB nanostructuring was mainly investigated by analysing cross-sections of the various structures. These cross-sections were also realised using the FIB. We tried several cross-sectioning techniques, milling of a hole with a sloped milling depth, line by line polishing and combinations. In the optimised method the first step is to locally deposit a layer of Pt using the FIB, in order to prevent redeposition. Secondly, a hole is milled with a sloped angle to avoid long milling times. Finally, a line-by-line scan (termed cleaning cross-section) is applied at a lower current (28 pA) to establish a high contrast image, as depicted in Fig. 1.

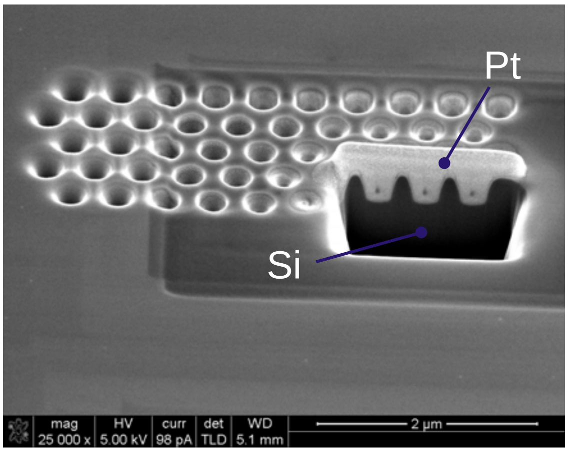

Fig. 1: Optimised cross-sectioning method used for investigation of the milled structures.

Since the electron-beam and the ion-beam columns have a fixed relative angle of 52°, angled SEM photos of the cross-section can be taken without rotating the stage. By tilting the substrate, the ion beam angle can be reduced for minimising the milling time of deep holes. Since the SEM photos are taken at an angle, the horizontal scale bar can not be applied to the vertical direction. The length of the image in vertical direction has to be scaled by 1/sin(angle).

Scanning procedures

In general, the first step in any FIB milling experiment is preparation of a mask file (stream file). This file contains all the information required by the machine in order to mill the desired geometry. Namely, the file contains series of pixels that define the structure and the milling time information for each pixel. The major difference between different scanning procedures is the sequence of each pixel, i.e. the order by which each pixel is milled. In a conventional raster scanning procedure, the ion beam sweeps the observed area line by line, as depicted in Fig. 2 (a) [7]. The ion beam is ideally turned on only on the pixel on which the geometry is defined and is off elsewhere. In practice, however, it is not completely off outside the desired areas, which in turn results in inter-hole milling. For the special case when the milled geometry has a circular cross section a spiral scanning routine may avoid the above mentioned shortcoming to a large degree. A schematic drawing of the spiral scanning procedure is given in Fig. 2 (b).

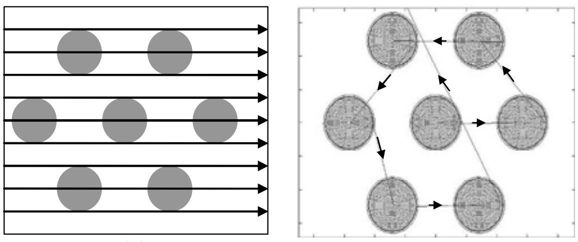

(a) (b)

Fig. 2: Schematic representation of the raster (a) and spiral (b) scanning methods. The beam is moving inside out in case of the spiral scan.

In order to compare the two types of the scanning procedures we have performed a series of experiments on Si. The sample was mounted on a holder by silver glue to ensure a conductive connection between the two. Two different stream files were designed for FIB milling. The common structure to be milled was chosen to be a 50-hole array with periodicity of 440 nm and hole diameter of 250 nm. There was a small difference in the number of pixels in the stream files due to the different file generation methods, which also caused minor difference in dose per hole for the two structures. Using a loop number of 12 for each method a milling depth of about 250 nm was obtained.

The results of the milling procedures using raster and spiral scanning are given in Fig. 3 (a) and (b), respectively. In order to be able to compare the two methods, we define two additional parameters, absolute height h_{abs} and relative height h_{rel}. The first one corresponds to the total height from the bottom of the hole to the surrounding silicon, while h_{rel} stands for the height difference between the bottom of the hole and the inter-hole sidewall. The side-wall angle φ is defined by the angle between the normal to the surface and the sloped side-wall around $h_{rel}/2$. The height of $h_{rel}/2$ of is also used as the reference point in the definition of the average hole diameter.

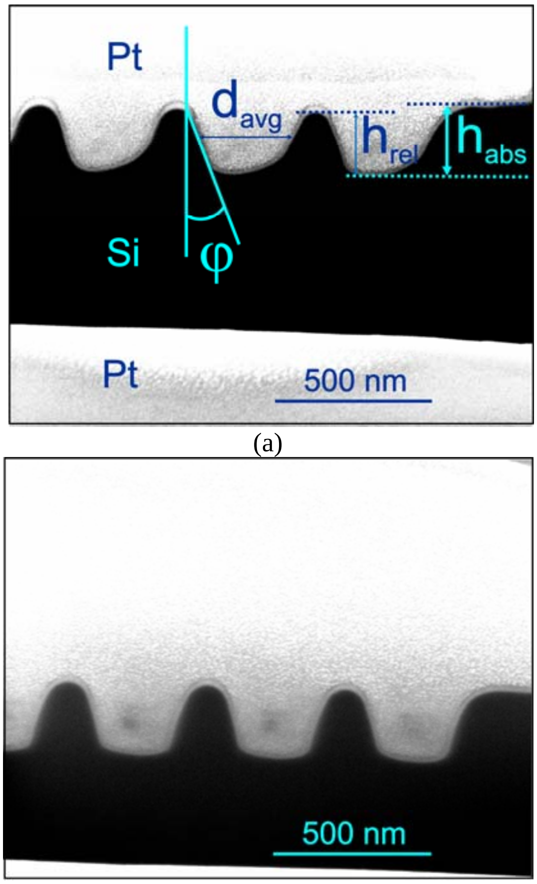

(a)

(b)

Fig. 3: Patterns milled at 48 pA using 12 loops and a dwell time per pixel of 0.1 ms. (a) Raster scan (b) Spiral scan.

Comparison of the cross-section profiles given in Fig. 3 clearly suggests that the holes are better defined by the spiral scanning method. It is evident that the absolute and relative heights in the two methods are different as expected from the different scanning strategies where in the raster scan method the sidewalls are scanned many more times than in spiral scanning. A further important difference between the structures fabricated by using the two methods is the difference between the side-wall angles in the case of raster scanning. This also results in an asymmetric cross-section of the holes. This effect is probably due to the redeposition effect that becomes significant when the beam is scanned in one direction. It is not observed in the case of spiral scanning which follows a more symmetric route, therefore minimizing the effects of redeposition.

As a result, in the course of FIB milling the spiral scan method reduces the amount of inter-hole milling significantly and results in better side-wall angles by reducing the effects of redeposition.

Dwell time variation

The redeposition can be influenced by changing not only the scan routine as shown in the previous section, but also by modifying the dwell-time parameters. Changing the dwell time in a scan pattern, leads to a change in required loop number to achieve similar milling depths.

We have performed two different studies in order to analyze this effect. In the first set of experiments the dwell time was kept constant at 0.1 ms while the loop number was steadily increased, resulting also in an increase of the dose per hole. The parameters are summarized in Table 1 and the analysis of sidewall angle variation with dose per hole used in the definition of the structure is plotted in Fig.4. The increase in the number of loops as the dwell time is increased also corresponds to increase in the ion dose per hole. It is evident from the figure that as dose per hole is increased in this case, the sidewall angle is reduced as desired.

To find the side-wall angle dependence on the dwell time, we kept the total dose applied to each hole constant. In this way the influence of the dose on the side-wall angle is separated from the dwell time dependency.

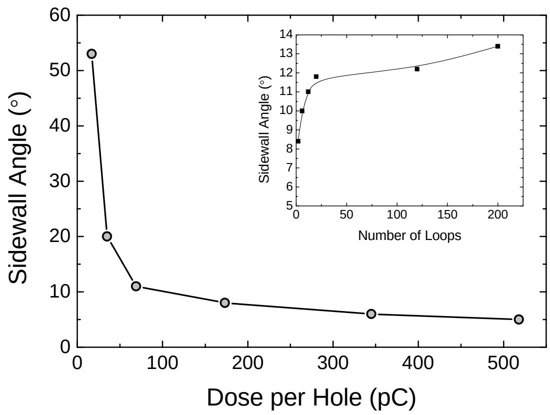

Fig. 4: Variation of the sidewall angle of hole structures as a function of number of loops

The dose can be kept constant by changing also the loop number when varying the dwell-time, i.e. keeping the product dwell time and the number of loops constant. The sidewall angle variation as a function of increasing number of loops is depicted in the inset of Fig. 4. Here, the increase in the loop number also corresponds to shorter dwell times. As a result, we can state that in order to obtain as small sidewall angles as possible one should choose a higher dose in combination with longer dwell time. However, this cannot be generalized for hole-sizes and doses other than studied here, because the geometry of the hole will specify the redeposition function and consequently the hole geometry.

Investigation of Gallium ion implantation

It is well known that ion beam milling in silicon can result in structures having high optical loss because of modifications of the crystalline Si induced by ion bombardment and implantation of for example Gallium ions within the sample. A possible route for achieving lower loss is by high temperature annealing. We have performed a preliminary investigation of the effect of Gallium ion implantation on optical loss of single-mode SOI channel waveguides. For that purpose we have exposed straight optical waveguides to the ion beam at six different doses between 5×10^{14} and 2×10^{17} ions/cm^2.

Table 1: Results of dwell time variation experiments.

Number of loops	Dose per hole (pC)	Absolute Depth, h_{abs} ±3% (nm)	Relative depth, h_{rel} ±3% (nm)	Average diameter, d_{avg} ±5% (nm)	Sidewall angle, ±5% (°)
3	17	83	68	310	53
6	35	160	141	290	20
12	69	320	292	261	11
30	173	872	766	220	8
60	345	1168	1065	222	6
90	518	1312	1224	217	5

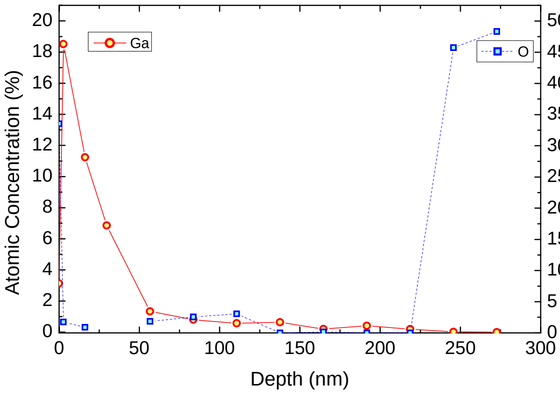

Fig. 5: Depth variation of gallium and oxygen atomic concentrations through SOI as measured by XPS.

For the smallest dose, the volume of the Si increases due to implantation; at higher doses we observe also Si removal by sputtering. The incorporation of Ga^+ ions in Si was analyzed by depth profiled XPS. A representative implantation profile is as given in Fig. 5. For a dose of 1×10^{17} ions/cm^2 we observe that almost all the gallium is within the first 50 nm of Si. We also observe the lower cladding's oxygen atoms as expected for the used SOI structure.

The optical losses were measured by using a customized setup that involves analysis of the scattered light with a linear infrared camera at a wavelength of 1.55 μm. A thermal annealing process was used in order to possibly reduce the optical losses. The preliminary results are plotted in Fig. 6.

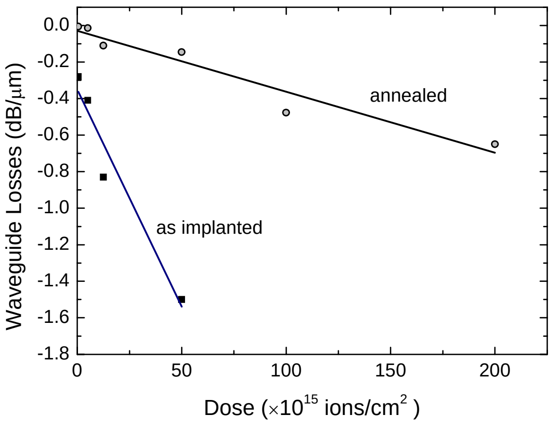

Fig. 6: Variation of measured waveguide losses with Ga ion implantation dose for both as-implanted and annealed single mode SOI waveguides.

For the as-implanted waveguides the optical losses are significantly higher and for the highest two doses there was no detectable propagation at all. As the samples were annealed at 800 °C for 60 minutes, light propagation improved by more than an order of magnitude.

The initial results discussed above suggest that further improvement is possible. The study towards minimization or elimination of the optical losses caused by gallium ion implantation while performing FIB milling is still ongoing.

Conclusions

We have investigated the technological difficulties in fabrication of sub-micron holes in silicon by using focused ion beam milling. Namely, we compared two FIB scanning procedures and showed the advantages of using a spiral scanning method for definition of holes in PCS structures. By investigating the parameters such as dwell time, loop number, and ion dose we determined the optimum FIB milling parameters.

Furthermore, we reported on the initial results on the effects of Ga^+ implantation during FIB milling on optical losses. We were able to reduce the propagation losses by more than an order of magnitude by thermally annealing the SOI waveguides.

Acknowledgments

This research was supported by NanoNed, a national nanotechnology program coordinated by the Dutch ministry of Economic Affairs, and was also supported by the European Network of Excellence ePIXnet.

References

1 Y. Akahane et al., Nature 425, p. 944, 2003.
2 Y.A. Vlasov et al., Nature 438, p. 65, 2005.
3 S. Reyntjens et al., J. Micromech. Microeng. 11, p. 287, 2001.
4 A.A. Tseng et al., Small 1, p. 924, 2005.
5 Y.K. Kim et al., IEEE J. Sel. Top. Quantum Electron. 11, p. 1292, 2005.
6 M.J. Cryan et al., IEEE J. Sel. Top. Quantum Electron 11, p. 1266, 2005.
7 Y.Q. Fu et al., Int. J. Adv. Manuf. Technol. 16, p. 877, 2000.